Chapter 10
Step Ultrasonic Motors

Great research progress for step USMs has been achieved since their invention more than 10 years ago. In 1991, Kusakabe developed a standing wave and self-correction USM[1], which made the USM succeed in step motion without feedback. Later, Miyazawa put forward a step USM[2-3] using a shifting standing wave mode based on Iijima's standing wave USM in 1993. Furthermore, in 1999, the author and Guiqing Wang, et al. designed and fabricated a new self-correction type USM[4-5]. In the same year, the author and Long Jin, et al. developed a mode rotary type step USM[6-7] with 80, 120, and 168 steps in one circle based on the theory proposed by Miyazawa. In 2000, Snitka designed an ultrasonic actuator[8] based on a linear USM using two modes, whose positioning accuracy reached nano-meter level. In 2003, Yong Jin, Jifeng Guo, et al. made a step USM[9] by combining a longitudinal mode and a torsional mode. In the next year, Xiangcheng Chu made a shaking-head type step USM[10]. In 2005, the author and Jiamei Jin, et al. developed a self-correction type step USM using modal rotation[11], a mode alternation type step USM[12-13], and a linear type step USM and a rotary type step USM using vibrator alternation[14-15]. Several prototypes were fabricated in different sizes for each type.

Compared to an electromagnetic step motor, the step USM has good characteristics, such as simpler structure, smaller size, better environmental adaptability, and no-electromagnetic interference[16]. It can be widely applied to optical devices, robotics, space shuttles, automatic control systems, military facilities, medical equipment and so on. The nano-meter step USM can also be used in electron beams, ion beams, X-ray, scanning electron microscope positioning, etc.

A step USM can be described as an ultrasonic motor which can realize the step motion with a certain step size.

USMs include two major types: a traveling wave and a standing wave, and these two types of USMs operate in two different ways. The traveling wave USM has good controllability, stability, and long life[17-22], while the standing wave USM has different performance and can realize movement with different forms[23-34]. Thus, many standing wave USMs are made by different operating modes and different driving schemes. The step USM is a significant branch of USMs. The step USMs can be divided into the adjustable steplength type and the fixed steplength type.

The adjustable steplength USM is driven step by step by switching on/off the driving signal in a carefully designed sequence. Its steplength is decided by the

C. Zhao, *Ultrasonic Motors*

width of the driving pulse[35]. When the USM starts or shuts down, fluctuations of the velocity will affect the uniformity of every step. When every step displacement is smaller, this fluctuation will be not negligible. In the condition of long-step and the multi-step positioning, the feedback loops have to be applied in order to reduce the position error.

The fixed steplength USMs possess some special structural forms to obtain step motion in the open-loop control[36]. This kind of step USMs has no accumulated error in multi-step operating. The single-step operating error is produced mainly from the machine work and assembly error.

10.1 Step Control of USM

An adjustable steplength USM is controlled by switching on/off the driving signal. Theoretically, the electromagnetic motors can also realize the step motion by similar operating, but the control is more difficult because the coil motor can not very quickly response to the control signal and can not make self-locking when its power is shut down. USMs possess characteristics of self-locking, rapid response and high position resolution. These naturally present advantages for the control of accurate step positioning.

USM's self-locking feature comes from the operating principle of friction drive. Usually, in the operating state, the contact area between the stator and rotor (or silder) is smaller than that in the non-operating state. Besides when it operates, there is also local sliding on the frictional interface, which makes USM's self-locking torque (or force) greater than the stalling torque (or the maximum output force). In other words, with the power shutdown, USM's rotor (or slider) will be quickly locked at the position where it arrives. This advantage is beneficial to the control of precision positioning.

The rapid response means the stator will soon achieve the steady state after power on. Namely, USM can reach its rating speed quickly.

USM's high positioning resolution is due to its micro vibration amplitude and high operating frequency. Generally, displacement in the sub-micron or nanometer level can be achieved when the stator makes the rotor (or slider) move in a vibration cycle.

Plenty of experiments show that large fluctuation of the positioning accuracy appears at the period of starting and ending the motor.

10.1.1 Startup and Shutdown Characteristics of USM

Under normal circumstances, in order to increase the amplitude and reduce the energy consumption, the driving frequency is designed to be close to the resonance frequency of the stator. In this way, the dynamic characteristics of USM is a key factor in precision positioning. The process, from the beginning of the stator's vibration to the accumulation of the energy and finally to its stable operating state, is called as the starting state of the motor. On the other hand, the

process, from the moment when USM's power is off and the stator obtains its own initial condition of vibration to the moment when the vibration of the stator stops completely and finally to states of shutdown the rotor (or slider), is called as state of shutdown of the motor. The intermediate state between these two states is the steady operating state of USM.

1. Stator's vibration response

According to the vibration theory described in Chap. 4, the forced vibration of the stator can be divided into three stages: ①a startup(beginning of an excitation); ②a steady state(keeping the excitation); ③an attenuation(switching the excitation).

Here, stage ① and ③ will be discussed because the vibration characteristics of these two stages directly relate to USM's response speed and positioning resolution. The Ref. [37] has analyzed the problem in detail and obtained the conclusion that the time for USM's stator vibrating in the stage ① and ③ is different. The difference between the two stages' time is mainly determined by damping of the stator. The greater the damping is, the bigger the difference will be. Generally, the damping of USM's stator is relatively small. So, the difference between the two stages' time is not large.

It is not enough to only consider the viscosity damping of the stator. In actual circumstance other damping factors still exist. From the point view of energy, it is valid that in the beginning of the forced vibration the damping prevents the system from accumulating energy. The greater the damping is, the longer the time t_s to reach the steady-state will be. In the decaying stage, the damping will consume energy. In other words, the greater the damping is, the sooner the decaying stage will be, the shorter the time t_e to stop the vibration will be. Consequently when the damping is bigger, the difference between the two stages' time $\Delta t = t_s - t_e$ will be greater.

2. The actual operating process of the motor

Corresponding to the vibration of the stator, the actual operating process of USM can be also divided into three stages: ①startup stage; ②steady operating stage; ③shutdown stage.

The characteristics of startup stage and shutdown stage for a typical traveling wave USM are shown in Fig. 14.12 and Fig. 14.13.

In the startup stage of USM, there is some delay, from the beginning of the vibration of the stator to the starting of the output of the rotor's shaft, which is called mechanical hysteresis of the motor. This is due to the whole system's damping and stiffness of the shaft coupling.

When the rotor is assembled, the boundary conditions of the stator will change. It's equivalent to adding the constraint to the stator, which increases its natural frequency and decreases its amplitude. When the stator's amplitude declines, the pre-pressure will increase the contact area on the contact interface between the stator and rotor at the same time. Not only the transmittability of the tangential force on the contact interface is increased, but also the area of sliding friction is increased, resulting in more energy dissipation. Thereby, the startup time increases with the increase of pre-pressure, while the shutdown time

decreases with the increase of pre-pressure.

The startup and shutdown characteristics for TRUM-45 under different pre-pressure are shown in Fig. 10. 1. It illustrates that the startup time increases with the pre-pressure going up while the shutdown time declines slightly with the pre-pressure rising up, as shown in Fig. 10. 1.

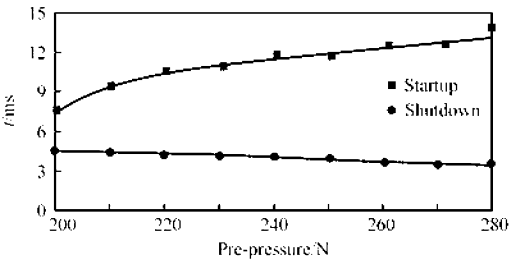

Fig. 10. 1 Startup and shutdown characteristics of TRUM-45 under different pre-pressure

10. 1. 2 Step Control for USM

Based on the preceding analysis, we can conclude that besides the load, other factors influencing the startup and shutdown time come from the motor itself. Among them the most unstable factor is the frictional interface between the stator and rotor. When the USM runs, the frictional properties at the interface will change from time to time due to wear, heating, and other reasons, which leads to fluctuation of the startup and shutdown time. These are the main reasons that make USM instability when it starts up or shuts down.

Figure 10. 2 shows test results regarding to the angular displacement versus the poweron time for TRUM-45. Fig. 10. 2(a) shows that the poweron time is 10ms, and the fluctuation of the displacement is large. It is primarily due to the startup time of the motor is about 8ms. Besides, there is the overswing, which needs about 30ms to make the speed relatively stable. The situation will be better when the poweron time more than 10ms, as shown in the Fig. 10. 2(b). The fluctuation reduces significantly and good linear relationship can be observed when the poweron time more than 100ms, as shown in Fig. 10. 2(c).

Another test is regarding to the motor's repeatability. As shown in the Fig. 10. 3, the USM was repeatedly tested 10 times. The maximal degree of decentralization based on the arithmetical mean value demonstrates that the shorter the poweron time is, the worse the repeatability is. When it turns in the counterclockwise direction, the degree of decentralization is lower than 10% if the time is more than 15ms. When it turns in the clockwise direction, the degree of decentralization is lower than 10% if the time is more than 25ms. For this USM, the difference of decentralization in the two directions is mainly caused by the speed difference in these two directions of the USM. Further, the degree of the decentralization shows the position error of the timing displacement. The

longer the electrical power is applied, the longer the step of the USM is, and the smaller the position error is.

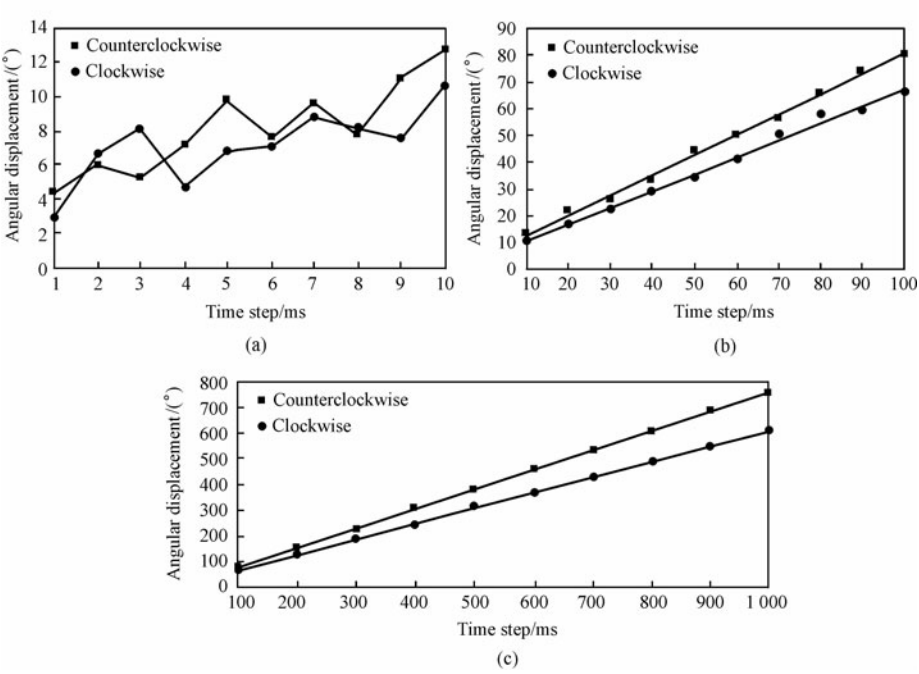

Fig. 10. 2 Testing curve of angular displacement of TRUM-45 vs. poweron time

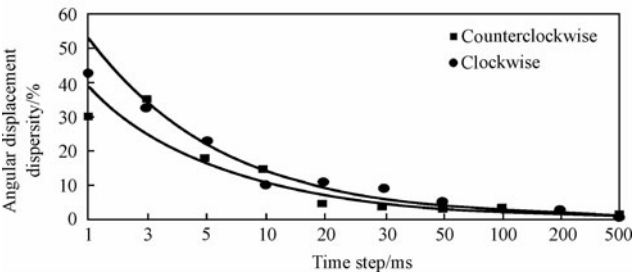

Fig. 10. 3 Testing curve on repeatability of angular displacement relating to poweron time for TRUM-45

The previous test shows that the USM's repeatability is bad in the startup stage. When the poweron time is more than 25ms during which the startup stage is completed, its repeatability of the displacement is acceptable. Thus, *the time relating to the designed step angle should be far more than the time of the startup stage when the motor is used for stepping positioning.*

1. Open-loop control method based on the poweron time as control variable

The size of the step and the positioning precision are relied on the startup and shutdown characteristics of the USM. As a result the exact data of the starting

and the decaying time are required, from which one can determine the relationship between the running time and the displacement.

Generally, there is a frequency automatic tracking technique for the USM, which can make operating speed stable. In the shutdown stage the slip friction mainly depends on the characteristics of the frictional interface, which can induce time-variability and uncertainty of the speed. Besides the problem of the slip friction, there are also other unstable factors such as the overshoot. However the time required for the whole stage of starting and ending is almost invariable. Hence, it is better that every time step includes the time for the starting or decaying stage to reduce the positioning error of every single step.

A micro control unit (MCU) is a unit used for controlling stepping movement. The starting time and decaying time and its corresponding angular displacement at different loads are obtained through the experiment in advance. These data are stored in the memory of the MCU in table format. When the MCU receives the instruction of the step pitch and the number of the step, which will be checked out with starting, ending time and the corresponding angular displacement accorded in the tables. At a certain rotational speed, the MCU will give the steady running time for every step and the corresponding control signal, which will control the operating time of a signal generator and a power amplifier so that the stepping motion of USM can be implemented.

Single-step running is showed in Fig. 10.4. The time for USM's startup is t_s, in which the angle that is rotated by the motor is θ_s. Similarly the decaying time is t_e, the angle rotated by the motor during t_e is θ_e. The angular speed and corresponding running time in steady state are $\dot{\theta}$ and t_p, respectively.

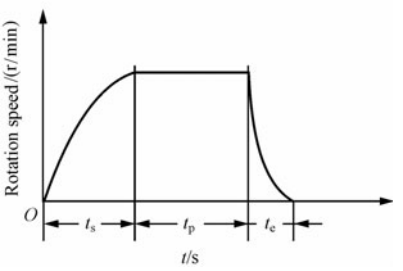

Fig. 10.4 USM's stepping motion controlled by poweron time

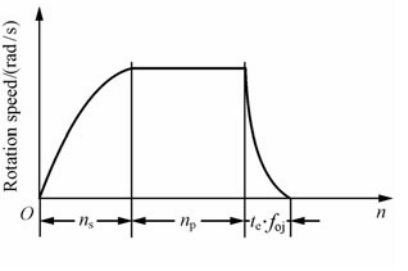

Fig. 10.5 USM's stepping motion controlled by number of excitation periodicity

If the motor's displacement of the ith step is θ_i, then the time used for the step should be

$$\begin{cases} t_i = t_s + t_p + t_e \\ t_p = \dfrac{\theta_i - \theta_s - \theta_e}{\dot{\theta}} \end{cases} \tag{10.1}$$

The poweron time is

$$t_i - t_e = t_s + \frac{\theta_i - \theta_s - \theta_e}{\dot{\theta}} \tag{10.2}$$

The minimum interval time between these two steps is t_e. The minimum step angle including a starting process and a decaying process is $\theta_s + \theta_e$. It is relevant to the rotational speed. The higher the speed is, the larger the step angle will be. Taking TRUM-45 as an example, the minimum step angle is about 15 degrees in the clockwise direction while in the counter-clockwise direction is about 20 degrees including the entire starting and decaying stage, and its corresponding positioning error is 10%.

2. Open-loop control method based on periodicity number of excitation as control variable

The open-loop control method based on the periodicity number of excitation as the control variable hopefully gets more position precise than that obtained by the previous open-loop control, and the differences mainly show in the process of shutdown. In the previous way, the driving signal hardly controls the motor to stop at the moment of the stator's vibration. This leads to the difference in the initial conditions when the stator starts the free vibration with damping. While nowadays, the exact initial conditions can be known. The similar initial conditions mean that the similar decaying time can be obtained.

This controlling method is similar to the first one. The periodicity number of the excitation for startup of the USM and its corresponding angular displacement and the decaying time and the corresponding angular displacement in different loads are obtained by experiments. Furthermore, the data are stored in the memory of DDS (Direct Digital Synthesizer) in data tables. When DDS receives the instruction of the step pitch and the number of step, which will check out the periodicity number of the excitation for startup and decaying of the USM and its corresponding angular displacement accorded in the tables. From the angular displacement relating to the single periodicity number of the excitation, DDS will give the periodicity number of the excitation for every step when the USM operates steadily. The step movement can be controlled by a power amplifier.

The periodicity of single step operating is shown in Fig. 10.5. It is assumed that the periodicity number of the excitation for startup of USM is n_s. During this period the rotational angle of the motor is θ_s. The shutdown time is t_e and corresponding rotational angle is θ_e, the stable angular speed is $\dot{\theta}$ and the operating frequency is f_{oj}.

If the angular displacement of the ith step is θ_i, the periodicity number of the excitation for this step is

$$\begin{cases} n_i = n_s + n_p \\ n_p = f_{oj}\left(\dfrac{\theta_i - \theta_s - \theta_e}{\dot{\theta}}\right) \end{cases} \tag{10.3}$$

The minimal time interval between the two steps is t_e. The minimal step angle is $\theta_s + \theta_e$ including the starting stage and decaying stage.

3. Closed-loop control method using the position sensors for feedback

The control precision of the open-loop control is primarily related to the stability of the startup and decaying processes of USM. Because of the poor stability, the feedback must be added to reduce the single-step displacement error and the accumulated error brought by the multi-step operating. A relatively direct approach is to utilize a position feedback.

Photo-electricity encoders or other position sensors can be used to acquire the location information. The informations acquired are then sent to the computers through the data acquisition card. The computer will cut off the driving signal in advance based on the built-in shutdown time t_e of the motor, so that the motor will stop in the target location. The control precision of this method is not relevant to the startup process of the motor, but primarily depends on the stability of both the shutdown process and the resolution of the photo-electricity encoder.

This method can get small step angle because it is not necessary to a complete startup process. However, it should be noticed that when the poweron time is less than startup time, the stator begins to enter the state of decaying from non-resonance of the stator with smaller amplitude and smaller speed. Different poweron time corresponds to different exciting state. The list of angular displacement relating to the different poweron time and poweroff time needs to be placed in the computer's memory in advance.

The stepping control is shown in Fig. 10.6. The shutdown time is t_e. During this period the turning angle of the motor is θ_e. The angular speed of the motor is $\dot{\theta}(t)$. The computer's instruction execution time is T after computer gives the instruction of shutting down the power. Namely, the computer will send the poweroff command when the motor is at a location $\theta = \theta_e + T\dot{\theta}(t)$ away from the target one. If the angular displacement of the ith step θ_i is required and during the startup time t_s the turning angle of the motor is θ_s, then the step angle θ_i can be written as

$$\theta_i = \theta_s + T\dot{\theta}(t) + \theta_e \tag{10.4}$$

From Eq. (10.4), θ_i can be reduced by decreasing θ_s, θ_e and $\dot{\theta}(t)$, and can reach a minimal step angle $(\theta_i)_{\min}$.

Previous three control methods can use a control strategy called DCM (Differential Composite Motion) to get a smaller step angle. Tsinghua University Xiangcheng Chu, Zengping Xing, et al. described this strategy[10], and fulfilled the step control in a shaking head type USM, whose diameter, length and operating frequency are ϕ15mm, 42mm and 30-45kHz, respectively. It's no-load speed is 150r/min, stall torque 0.12N·m, startup time 0.24ms, and minimum step angle 12″.

The step angle θ_i can be obtained by the way of turning forward and backward. As shown in Fig. 10.7, the every step contains two processes: one is starting forward, running and decaying; the other is starting backward, running and decaying. There are some advantages in this way: the smaller step angle and greater output torque can be obtained. The displacements in the two startup and deca-

ying processes can be subtracted with each other, which can reduce the error from instability state. But the way is forbidden when the overshot is not allowed.

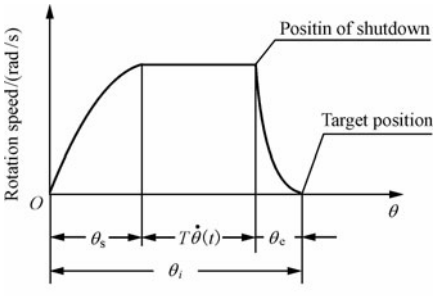

Fig. 10. 6 Stepping motion of USM using closed-loop control

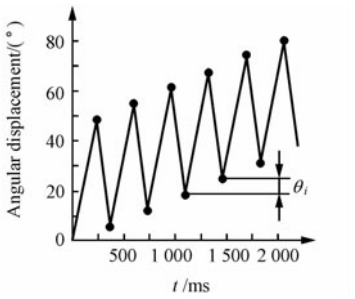

Fig. 10. 7 DCM's locating strategy of stepping

10. 1. 3 Factors Impacting on Single-step Positioning Accuracy

For the step USM, the single-step displacement accuracy depends on its stability including the stability of stator's vibration and the force transferring to friction interface at different time and in different environment.

1. Stability of stator's vibration

The main factor influencing the stability of stator's vibration is the change of connecting performance between the stator and piezoelectric ceramics. At present, there are three ways to connect a stator with a piezoelectric ceramics: compacting way, welding way and bonding way.

(1) Compacting way

Compacting way is conducted by a clamping force induced with connecting bolt, which makes both the modal frequency and amplitude sensitive to the clamping force. When USM is running, the heat from both the piezoelectric ceramic pieces and the friction interface will cause the stator's temperature rise. Due to thermal expansion the clamping force changes, then results in the fluctuation of the stator's modal frequencies and amplitudes. In addition, after long running, the motor's rated speed will change. Generally, the piezoelectric constant d_{33} is bigger than its d_{31}, and the clamping method is more suitable for these transducers that take the d_{33} piezoelectric effect, such as an ultrasonic motor using longitudinal-torsional bybrid vibration (see Chap. 8).

(2) Welding way

Welding way is the method that joins piezoelectric ceramic pieces and a stator under a high temperature, which is beneficial to more effectively transfer piezoelectric ceramic deformation to the stator; further, it can provide high excitation efficiency along with decreasing mechanical hysteresis. In addition, the welding possesses high reliability and stability, and the performances of USM are preferable. However, in general, with the stator vibration, the strain of the piezoelectric ceramic pieces on the welding surface and the strain of the stator surface are

not totally consistent. This leads to a localized stress concentration when USM is running, and the welding layer will has fatigue failure.

(3) Bonding way

Bonding way is the method of which water glue cement and so on bond a piezoelectric ceramic pieces to a stator in certain temperatures and pressures. Currently, an epoxy resin and acrylic adhesive is used extensively for USM. The adhesive possesses sufficient strength, which can provide the elastic link between the stator and piezoelectric ceramic pieces and release the stress concentration on the bonding surface. Mostly this approach can be just utilized for the d_{31} piezoelectric effect. Beside the thickness of the adhesive layer has great effect on the excitation efficiency, temperature change also affect the elasticity of the layer.

Comparatively, the welding way and bonding way can make USM operating stable, while compacting way can induce some unstability.

2. Stability of friction interface

Good performance of the friction interface can enhance the torque or the running velocity of USM. A moderate friction coefficient, high hardness and high wearability are the basic requirements for the friction interface.

The stability of the friction interface is affected by the factors including the characteristics of friction materials, the surface morphology of the interface and the changes of the tribopair to environment, such as temperature, humidity, and vacuum (see Chap. 3).

The stability of friction interface is a key to achieve the stable step interval of the step USM. The wear and tear of the tribopair change operating condition.

From analysis above, we can draw the following conclusions: applying the materials with a moderate friction coefficient, high hardness and high wearability is beneficial for obtaining more stable friction interface.

10.2 Step USM with Fixed Steplength

10.2.1 Standing Wave USM Used for Constructing Step USM

The standing wave USM discussed in this section is a type of rotational USM whose stator is ring shape, as shown in Fig. 10.8. There are 4 teeth distributed equally on the ring stator. The rotor is pressed on it by the pre-pressure provided with a spring. The monodirectional polarized piezoelectric ceramic ring has 8 uniform electrodes, as shown in the Fig. 10.9.

Figure 10.10 is a diagram expanded in the circumferential direction of the USM. The figure shows that the stator's mode can be excited by the driving voltage. This mode is the standing wave $\phi(\theta)$.

In the coordinate of Fig. 10.10, the standing wave can be expressed as:

$$\begin{aligned}\phi(\theta) &= w_0 \sin(\omega t + \varphi)\cos(k\theta - k\alpha) = w_0 \cos k\theta \cos k\alpha \sin(\omega t + \varphi) \\ &\quad + w_0 \sin k\theta \sin k\alpha \sin(\omega t + \varphi) = \phi_1(\theta) + \phi_2(\theta)\end{aligned} \tag{10.5}$$

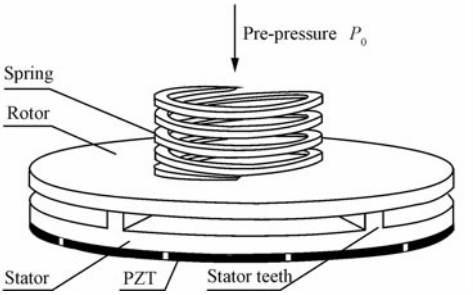

Fig. 10. 8 Basic structure of rotation USM using standing wave

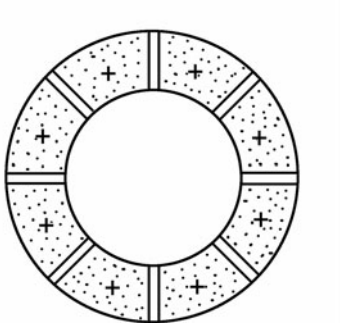

Fig. 10. 9 Piezoelectric ceramic's subareas of uniform electrodes of rotary USM using standing wave

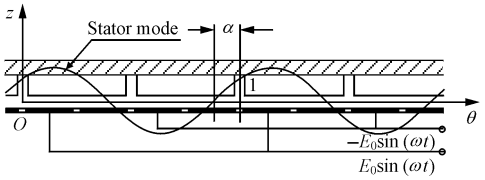

Fig. 10. 10 Operating mode of standing wave type rotatory USM

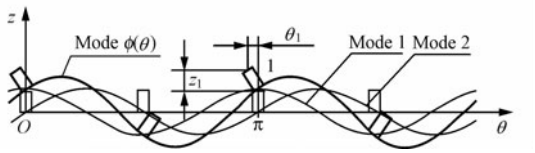

Fig. 10. 11 Decomposition of stator's operating mode

Where $\phi_1(\theta) = w_0 \cos k\theta \cos k\alpha \sin(\omega t + \varphi)$, $\phi_2(\theta) = w_0 \sin k\theta \sin k\alpha \sin(\omega t + \varphi)$, k is the number of the standing wave in the stator, and here $k = 2$. $\phi_1(\theta)$ and $\phi_2(\theta)$ are two standing waves whose phase difference is $\pi/2$ decomposed from $\phi(\theta)$ in the space. Moreover they are called as the mode 1 and mode 2, respectively, as shown in Fig. 10. 11.

If teeth are taken as rigid, teeth's movement will be determined by the rotational and translational movement of the points on the neutral layer of ring which is in the bending vibration. In this figure, the tooth No. 1 lies in the location of $\theta = \pi$. The movement of the point on the neutral layer of the ring in the z direction is

$$\phi(\theta)|_{\theta=\pi} = \phi_1(\theta)|_{\theta=\pi} \tag{10.6}$$

The teeth's translational movement is determined by mode 1. That is to say, the point's angle of rotation is

$$\gamma = \arctan \frac{\partial \phi(\theta)}{r \partial \theta}\bigg|_{\theta=\pi} = \arctan \frac{\partial \phi_2(\theta)}{r \partial \theta}\bigg|_{\theta=\pi} \tag{10.7}$$

Teeth's rotary movement is determined by mode 2. Where r is the stator's outer diameter.

It is valid to assume that the distance between one point on the top of tooth No. 1 and the neutral layer of the ring is h, and then the movement of this point in the θ direction is

$$\theta_1 = \frac{h}{r}\sin\gamma \approx \frac{h}{r}\frac{\partial \phi_2(\theta)}{r\partial\theta}\bigg|_{\theta=\pi} = \frac{h}{r^2}k w_0 \sin(\omega t + \varphi)\sin k\alpha \qquad (10.8)$$

Movement of this point in the z direction is

$$z_1 = \phi_1(\theta)\bigg|_{\theta=\pi} + h(1-\cos\gamma) \approx \phi_1(\theta)\bigg|_{\theta=\pi} = w_0 \cos k\alpha \sin(\omega t + \varphi) \qquad (10.9)$$

From the deduction above, the mode 1 makes the tip of the tooth to move in the z direction, while the mode 2 makes the tip of the tooth to move in the θ direction. Further, z_1 and θ_1 correspond to the point's amplitude of the tip of the stator tooth in the z and θ direction, respectively.

Giving the pre-pressure, an excitation voltage and height of teeth, the angle α become the key indicator determining the synthesis of displacements. As the angle α changes, the wave shape formed by the tip's movement is decided. The angle α can be determined from design requirement so that the polarized pattern of piezoelectric ceramic ring can be determined.

The wave shapes of $\phi_1(\theta)$ and $\phi_2(\theta)$ as the α changes are shown in Fig. 10.12.

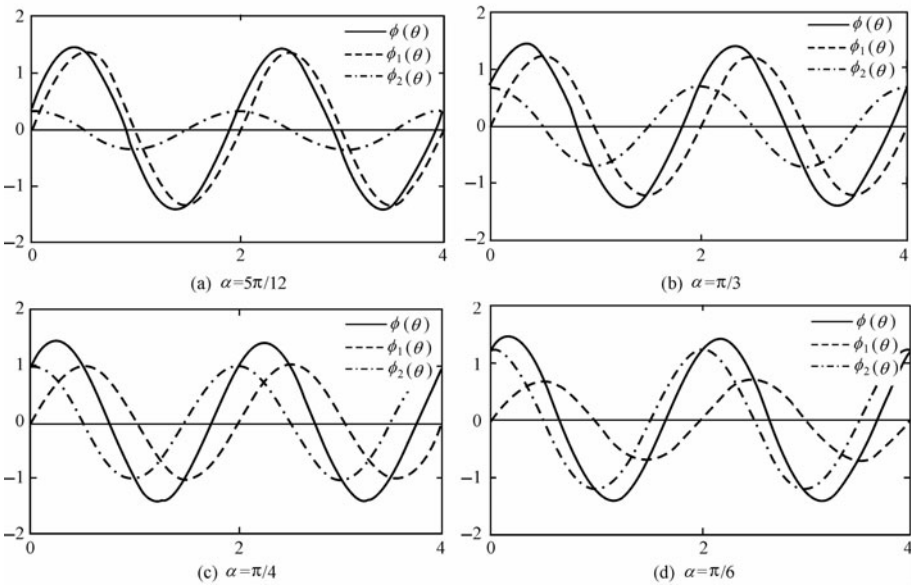

Fig. 10.12 Decomposition of standing wave with different α

When $0 \leqslant \alpha \leqslant \pi/4$, the amplitude of horizontal movement is larger than the

one of vertical movement; when $\pi/4 \leqslant \alpha \leqslant \pi/2$, the latter is larger. The shape of the locus is determined by h and α. When the designer needs bigger torque, it's better to make z_1 larger. If the designer needs bigger speed, it's better to make θ_1 larger.

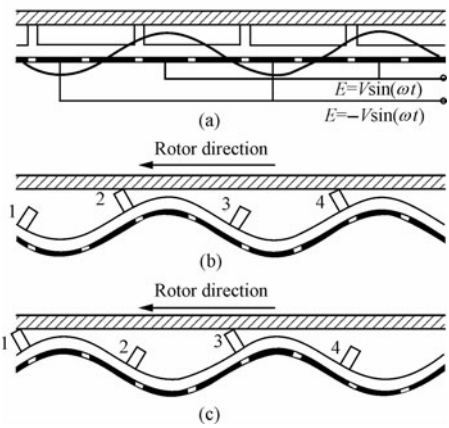

Fig. 10. 13 Operating principle of rotor rotation in anticlockwise

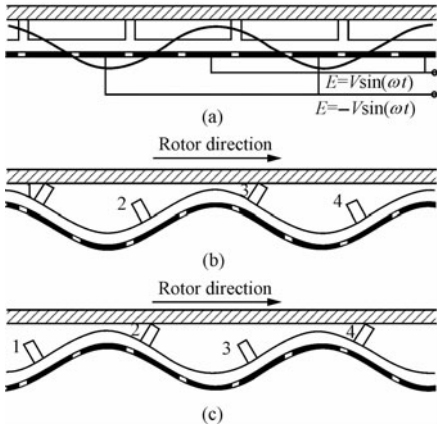

Fig. 10. 14 Operating principle of rotor rotation in clockwise

Figure 10. 13(a) shows an operating shape produced by the annular plate type stator when a single phase voltage E excites the stator. Two of the four teeth of stator move in counterclockwise and contact with the rotor. The friction between the stator and rotor drives the rotor turning in counterclockwise. The other two teeth move in clockwise. Because they located close to the trough and do not contact with the rotor, then they cannot push the rotor. In the first half cycle of the stator's vibration, the teeth No. 2 and No. 4 contact with the rotor and drive the rotor, as shown in Fig. 10. 13(b). In the second half cycle of the stator's vibration, the teeth No. 1 and No. 3 contact with rotor and drive the rotor, as shown in Fig. 10. 13(c).

Figure 10. 14 shows the driving voltage which makes the rotor turn reversely. The vibration mode is shown in Fig. 10. 14(a). The moving decomposition of the teeth's tip and the rotor rotation are shown in Fig. 10. 14(b) and Fig. 10. 14(c).

10. 2. 2 Modal Rotary Type Step USM

1. Structure of USM

The structure of a modal rotary type step USM is basically the same as the previous standing wave type USM. It is made of the annular stator, piezoelectric ceramic ring, spring and rotor. The difference is that the teeth are on the rotor instead of on the stator, as shown in Fig. 10. 15.

2. Driving mechanism

The stator has a mode B_{0k} excited by the piezoelectric ceramic ring. According to thin plate vibration theory, the displacement of point P on the stator's surface in

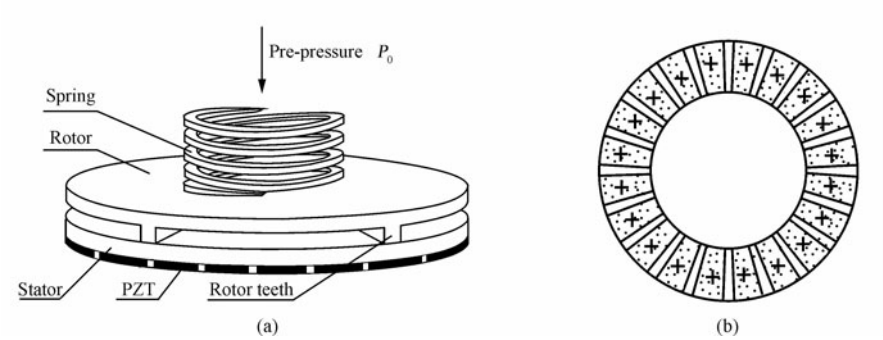

Fig. 10. 15 Basic structure of modal rotary step type USM and electrodes of piezoelectric ceramic ring

the z direction can be expressed as

$$w_P(r,\theta,t) = R(r)\sin(k\theta)\sin(\omega t) \tag{10.10}$$

The speed of point P along the θ direction can be expressed as

$$V_s = \dot{\theta}_P(r,\theta,t) = \frac{d}{2}k\,\omega\,R(r)\cos(k\theta)\cos(\omega t) \tag{10.11}$$

where d is the thickness of the plate, k is the number of the wave, ω is the driving angular frequency, r is the radial coordinate of the point, and $R(r)$ is the Bessel function

$$R(r) = AJ_n(kr) + BY_n(kr) + CI_n(kr) + DK_n(kr)$$

Where $J_n(kr)$ and $Y_n(kr)$ are the first and second type nth order Bessel functions, respectively; $I_n(kr)$ and $K_n(kr)$ are the first and second type nth order corrected Bessel functions, respectively.

The rotor motion is acquired by two actions from the contact of the stator with rotor. One is the motion of the points on the stator's surface, and the other is the circumferential component force at the contact points of the stator with rotor. From Eq. (10.11), the speed V_s of point P along θ direction, which locates at the stator's surface between the wave crest and nodal diameter, changes within the cycle of the stator's vibration, as shown in Fig. 10.16. In the first quarter of the cycle of the stator's vibration (namely, $\omega t = 0\text{-}\pi/2$, as shown in Fig. 10.16a) or the fourth quarter (i.e. $\omega t = 3\pi/2\text{-}2\pi$, as shown in Fig. 10.16(d)), the speed V_s direction aims at the nodal diameter of the mode shape. In the second quarter (i.e. $\omega t = \pi/2\text{-}\pi$, as shown in Fig. 10.16(b)) or in the third quarter (i.e. $\omega t = \pi\text{-}3\pi/2$, as shown in Fig. 10.16(c)), the speed V_s direction aims at the crests (or trough) of the mode shape. If there is no relative sliding on the contacting surface between the stator and rotor, the rotor will acquire the momentum in the circumferential direction that depends on the contacting period between the rotor's teeth and stator.

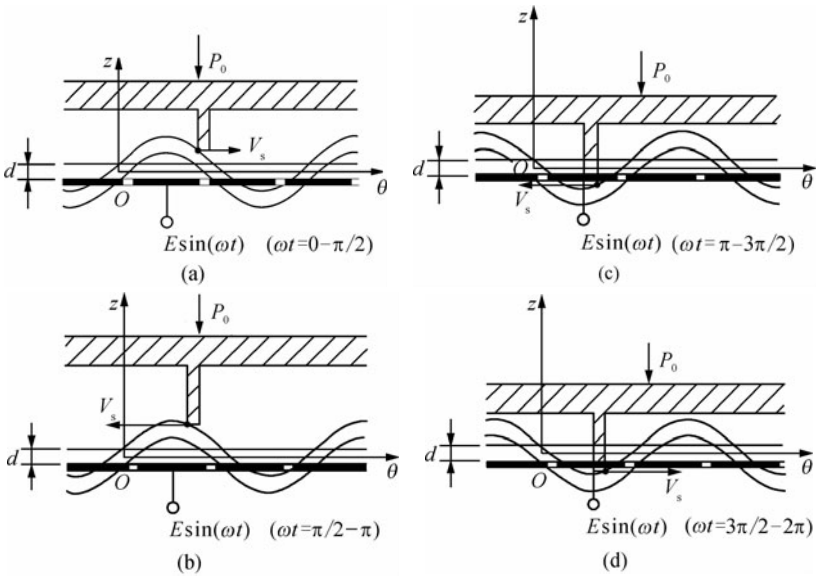

Fig. 10. 16 Speed component V_s of contact point on stator along circumferential direction

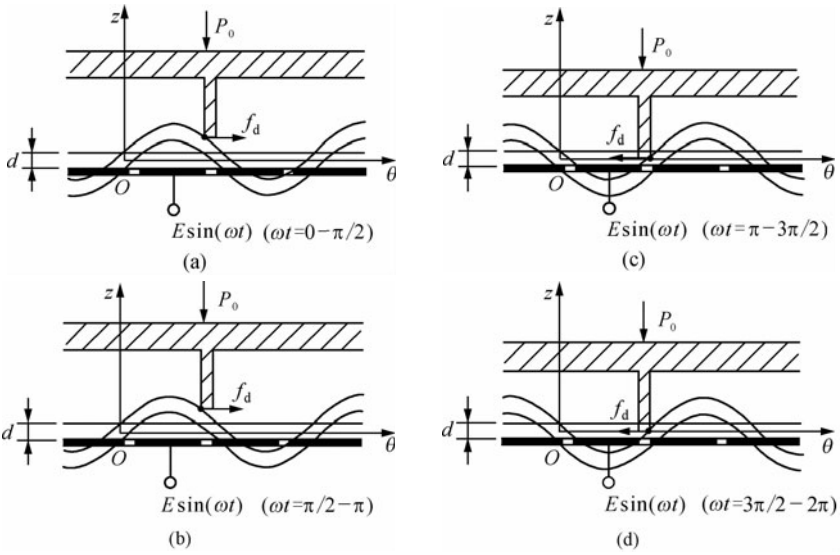

Fig. 10. 17 Force component f_d of contact point on rotor along circumferential direction

The force f_d in the circumferential direction is caused by the changing the slope on the contacting surface of the stator with rotor under the pre-pressure P_0. The direction of the force f_d also changes during the cycle of the stator's vibration, as shown in Fig. 10. 17. In the first quarter of the cycle of the stator's

vibration (i. e. $\omega t=0\text{-}\pi/2$, as shown in Fig. 10. 17(a)) or in the second quarter (i. e. $\omega t=\pi/2\text{-}\pi$, as shown in Fig. 10. 17(b)), the force f_d direction aims at the nodal diameter of the mode shape. In the third quarter (i. e. $\omega t=\pi\text{-}3\pi/2$, as shown in Fig. 10. 17(c)) or the fourth quarter of the cycle of the stator's vibration (i. e. $\omega t=3\pi/2\text{-}2\pi$, as shown in Fig. 10. 17(d)), the direction of the force f_d aims at the trough or crests of the vibration shape. If there is relative sliding on the contacting surface between the stator and rotor, the rotor will be driven by the circumferential force component f_d whose direction depends on the contacting period between the rotor's teeth and the stator.

If the rotor only contacts with the stator during the first quarter of the cycle of the stator's vibration, which can assure that the motion component V_s has the same direction with the force component f_d. In fact, if the number of teeth on the rotor is as twice as that of the nodal diameters, the stator will contact with the rotor in the first quarter or the second quarter of the vibration, i. e. $\omega t=0\text{-}\pi/2$ or $\omega t=\pi/2\text{-}\pi$, as shown in Fig. 10. 18.

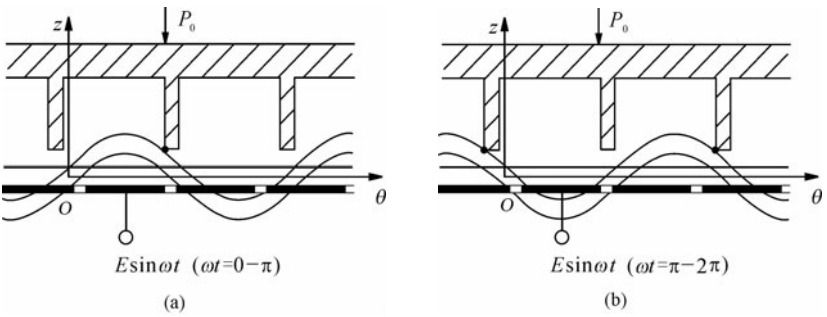

Fig. 10. 18 Contact points between the stator and rotor

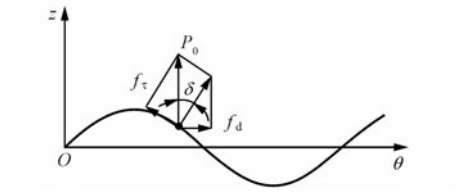

Fig. 10. 19 Force analysis of rotor's teeth

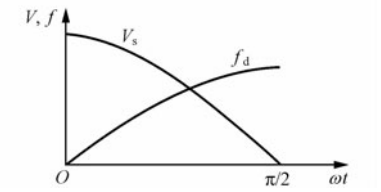

Fig. 10. 20 Relationship of V_s and f_d vs. time

Assuming that the rotor contacts with stator during the first 1/4 cycle of the vibration, the circumferential component f_d induced by contacting the stator with rotor teeth under the pre-pressure P_0 can be expressed as

$$f_d = P_0\cos\delta\sin\delta = \frac{P_0}{2}\sin 2\delta$$

$$\tan\delta = \frac{1}{r}\frac{\partial z(r,\theta,t)}{\partial\theta} = k\frac{R(r)}{r}\cos(k\theta)\sin(\omega t)$$

Considering that δ is small, there is an approximate relationship, as shown in Fig. 10.19

$$\sin 2\delta \approx \tan 2\delta = \frac{2\tan\delta}{1-\tan^2\delta} \approx 2\tan\delta$$

Thus

$$f_d \approx P_0 \tan\delta = P_0 k \frac{R(r)}{r}\cos(k\theta)\sin(\omega t) \qquad (10.12)$$

The changes of V_s and f_d versus time t are shown in Fig. 10.20. In the period of the contact, the circumferential movement of the points on the stator's surface contributes to drive the rotor; while in the anaphase of the contact, the circumferential force component produced by contacting both the stator and rotor teeth under the pre-pressure will also drive the rotor more effectively. Thereby, the design on the contact period of the stator with rotor is directly related to the design of frictional features of the contacting interface.

The friction coefficient that is big enough can make the horizontal movement of the points on the stator to transmitted reliably to the rotor; the small friction coefficient make the stator and rotor teeth to possess relative slide under the pre-pressure, so that the circumferential force component F_d can come into better use for the driving force.

It is impossible to design two friction materials with friction coefficients on the same surface, and only one of driving methods can be chosen to design the motor:

(1) Use horizontal movement of the points on the stator surface to drive the rotor, which has large enough friction coefficient.

(2) Use the circumferential component force under pre-pressure between the stator and the rotor's teeth to drive the rotor, keeping the friction coefficient as small as possible.

3. Stepping principle

Modal rotary type step USM relies on the vibration of the stator ring to make the rotor stepping. As shown in Fig. 10.15, the piezoelectric ceramic ring is polarized in one way in the axial direction. The number of electrode is 20. Four teeth are distributed on the rotor uniformly, and B_{02} is the operating mode. On the purpose of convenient observation, the stator and the rotor are expanded along circumferential, as shown in Fig. 10.21.

The sinusoidal voltage is utilized for the electrodes of the piezoelectric ceramic ring, as shown in Fig. 10.21(a). The bending standing wave B_{02} of the stator is excited. The rotor's teeth move forward to the stator's nodal diameter under the effect of the stator, as shown in Figs. 10.21(b) and (c). When the rotor's teeth locate at the nodal diameter, as shown in Fig. 10.21(d), the first step of the motor's movement will be over. When the step is finished, the power is supplied to the electrodes of the piezoelectric ceramic ring. From Fig. 10.21(e), the bending standing wave B_{02} of the stator is excited again, but at this time the standing wave has turned $2\pi/20$ arcs around the motor's shaft . The rotor's teeth moves forward to the stator's nodal diameter, as shown in Figs. 10.21(f) and (g).

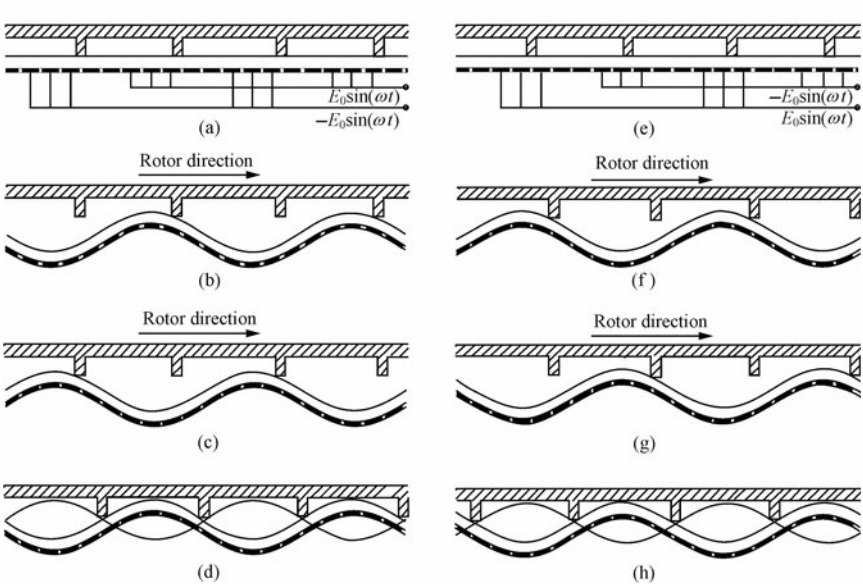

Fig. 10. 21 Moving decomposition for modal rotary type step USM

When the rotor's teeth locate at the nodal diameter of the stator, as shown in Fig. 10. 21(h), the second step of the motor's movement will be finished. Furthermore, changing connecting pattern of electrodes the power can make the standing wave turn step by step, and drive the rotor stepping, whose step angle is $2\pi/20$ arc.

4. Step number and steplength

In fact the minimum step angle of the motor is the minimum angle θ which is the turning angle of the standing wave in the stator. The most step number of the rotor turning in one cycle is $N = 2\pi/\theta$, which relies on the wave number k of the standing wave, the electrode number m_p, and the electrode number m_e applied power. Next the mode B_{0k} is discussed as an example to explain the relationships between these parameters.

If the operating mode of the stator is B_{0k}, the wave number of the stator's circumferential wave is k and the wave length is $\lambda = 2\pi/k$. The number of rotor's teeth is less than or equal to $2k$. In order to make all points near each nodal diameter to drive the rotor, the number of the rotor teeth is $2k$ for the best. In order to excite effectively the bending mode, the angle of each sector area should be less than half of a wavelength, i. e.

$$\theta_e < \frac{1}{2}\lambda \tag{10.13}$$

The number of the electrodes should satisfy

$$m_p > \frac{2\pi}{\theta_e} > \frac{4\pi}{\lambda} = 2k \tag{10.14}$$

If each crest or trough of the standing wave all can be excited by one corresponding sector area, it can be called as a "pure" mode excitation. Here, the number of the group is $m_e = 2k$, and this approach requires the number of electrode is $m_p = 2jk$ (j is the natural number), which means m_p is $2j$ times of the number k of the stator's circumferential wave. In such circumstances, the step angle is $\theta = 2\pi/m_p$. As shown in Fig. 10.22, B_{04} mode, the number of the group is $m_e = 8$; the number of the electrodes is $m_p = 40$; the step angle is $\theta = 2\pi/40$ and the number of the steps is $N = m_p = 40$.

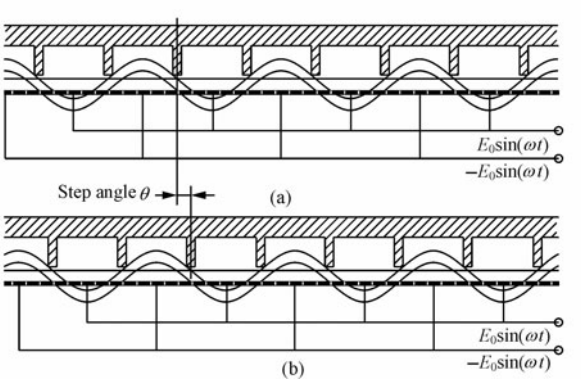

Fig. 10.22 A "pure" mode excitation method

The smallest step angle using the "pure" mode excitation method is only determined by the number of the sector areas (electrodes). Due to the restrictions of mechanical process, this approach will obtain a larger step angle as well as a smaller number of steps.

The other excitation method is the non-pure mode excitation one, which means the number of group satisfies $m_e < 2k$. In this way, the same step angle can be received with less group. However, the number of group is reduced, and the problems arising from it is that the utilization for piezoelectric ceramics declines and the output power is less . The relationship between the numbers of steps, the group and electrodes can be expressed as

$$N = 2k\frac{m_p}{m_e} \tag{10.15}$$

For the smallest step angle

$$\theta = \frac{2\pi m_e}{2k\,m_p} = \frac{\pi m_e}{k\,m_p} \tag{10.16}$$

An example is of the B_{04} mode: the number of group $m_e = 2$, the number of electrodes $m_p = 10$, the step angle $\theta = \pi/20$ and the number of steps $N = 40$.

5. Design of modal rotary type step USM

Figure 10.23(a) is an assembly drawing of the 80-step motor. No. 01, 02, 03, and 04 are a rotor, rotor teeth, stator, and piezoelectric ceramic ring, respectively. The outer diameter, inner diameter, and thickness of the stator are

60mm, 45mm, and 3mm, respectively. Fig. 10.23(b) is the piezoelectric ceramic ring attached on the back of the stator, whose outer diameter, inner diameter, and thickness are 60mm, 45mm, and 0.5mm, respectively.

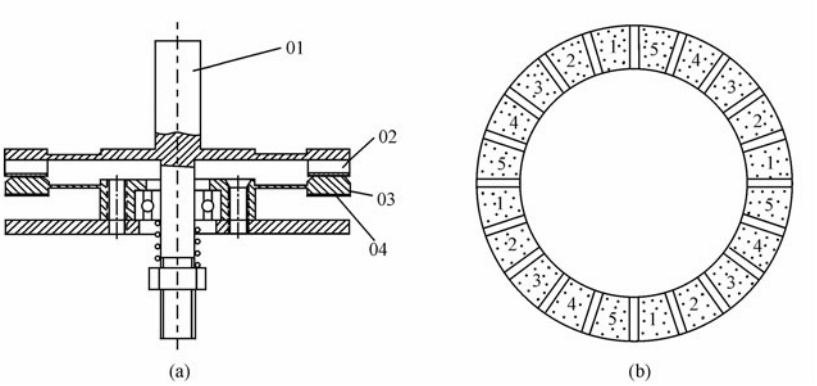

Fig. 10.23 80-step motor (a) and electrodes of piezoelectric ceramic ring (b)

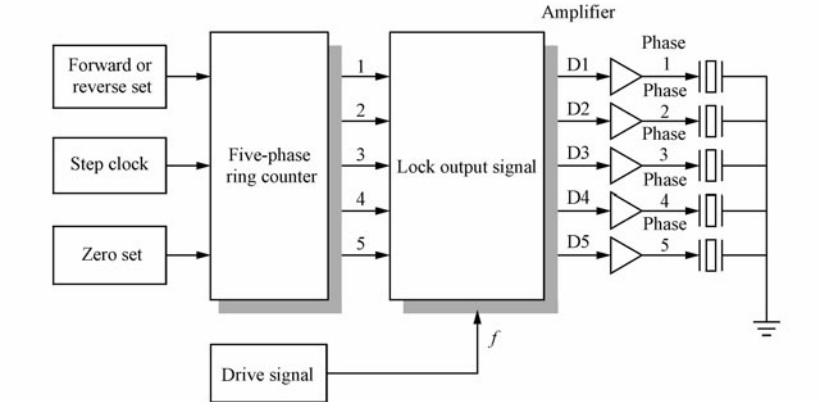

Fig. 10.24 Schematic diagram of five-phase drive circuit

The ceramic ring is evenly divided into 20 sector areas (namely $m_p=20$, which all are polarized in one direction). The sector areas are divided into 5 groups, which are marked the number 1, 2, 3, 4, and 5. Then each group has 4 sector areas, namely $m_e=4$. The step number is N=80, and the step angle $\theta=2\pi/80$. The step motor is known as the rotary step USM with five phases and 80 steps.

Figure 10.24 shows the element block diagram of the drive circuit for the rotary step USM with five phases and 80 steps. Fig. 10.25 presents an actual driving circuit schematic. The five phases drive signals are from a PWM controller TL494 (controlling the output voltage through adjusting pulse width), and the output frequency of the drive signal is close to the resonant frequency of the stator. The five-phase ring counter is composed of two four-ring counters 40194. The stepping clock is controlled by chip 555. The output signal of the five-phase

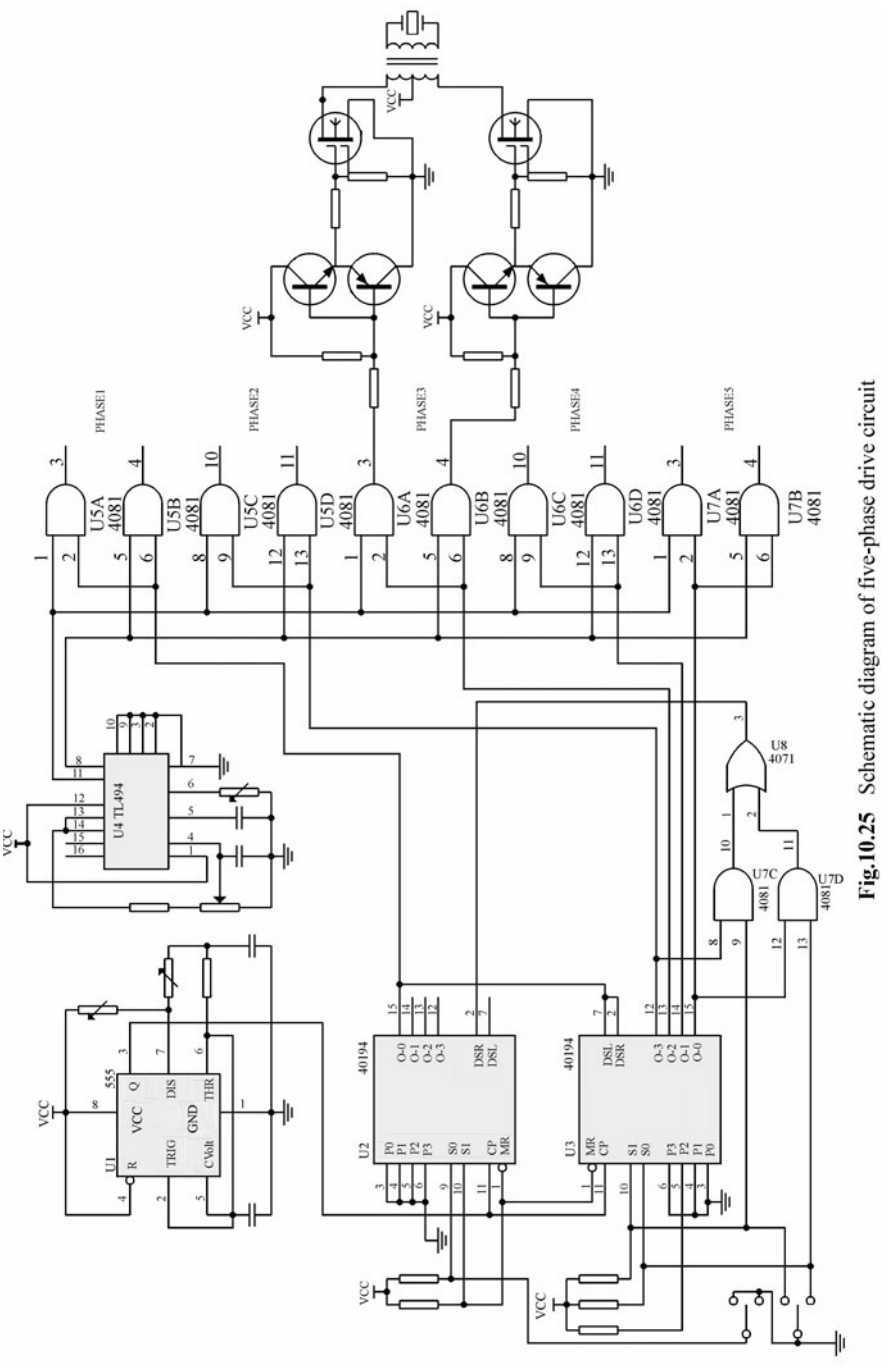

Fig.10.25 Schematic diagram of five-phase drive circuit

ring counter through the gate circuit transmits the drive signals to the push-pull control circuit terminal.

Figure 10. 26 shows the measured results of angle displacements when a rotary step USM with five phases and 80 steps is rotating in the two opposite directions. The maximum error of the step angle is about 0. 7°. After running 800 steps, the ultimate angular error is no more than 0. 7°.

In the case of load-free, the maximum speed of the step USM is 6. 25r/min, when the drive time of each step is not less than 0. 2 second. The maximum output torque of the USM is 0. 068N•m

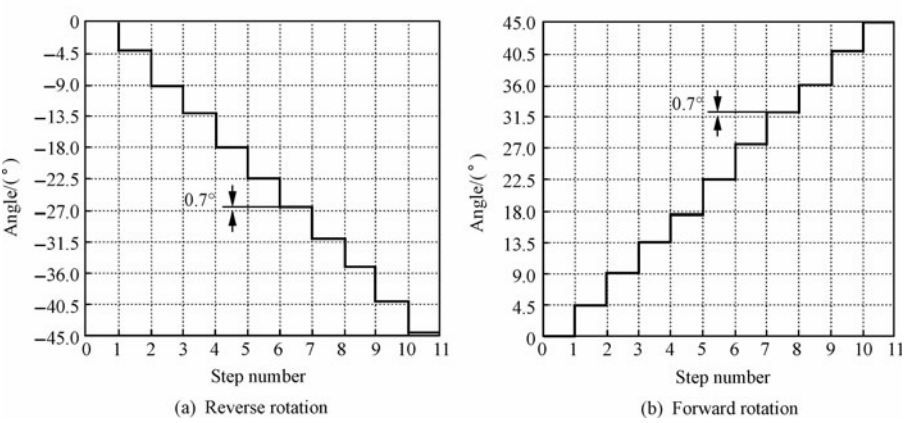

Fig. 10. 26 Step angular displacement measurement of a step USM with five phases and 80 steps at forward rotation or backward rotation

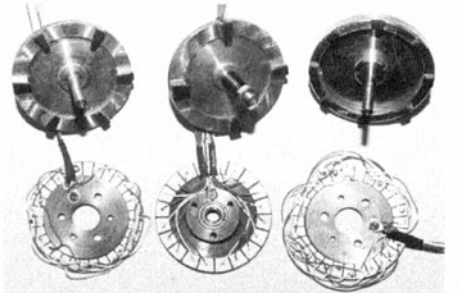

Fig. 10. 27 Rotors and stators of mode rotary type step USM

Fig. 10. 28 Mode rotary type step USM using 5-phase driver

Figure 10. 27 shows the stators and rotors of the rotary type step USMs with a 80-step, a 120-step, and a 168-step[6-7] designed by the author, long Jin, et al. Fig. 10. 28 shows a step USM using a 5-phase driver.

6. Features

By modal rotation and changes of nodal diameter location, this kind of motors makes rotor teeth move to the nodal line and drives rotor to movement step by

step. There is no accumulation of errors because it is from certain modes corresponding to the rotor position.

10.2.3 Self-correction Peak Type Step USM

A self-correction peak type step USM realizes its step motion by switching its two operating states: standing wave driving and self-correction positioning.

1. Structure and driving mechanism of the motor

The structure of self-correction peak type step USM is similar to the aforementioned standing wave type one. It is made of a stator, piezoelectric ceramic ring, spring and rotor. The difference is that the rotor has some radial slots, as shown in Fig. 10.29.

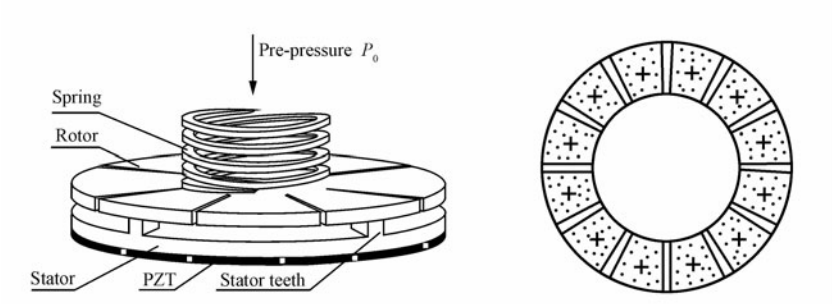

Fig. 10.29 Self-correction (tuning peaks) type step USM's structure (left) and electrodes (right)

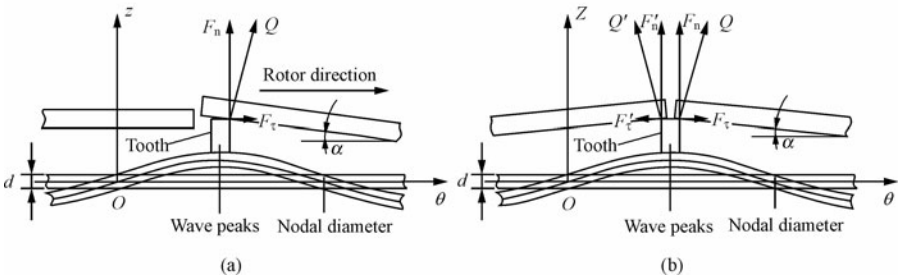

Fig. 10.30 Self-correction mechanism of self-correction peak type step USM

This type of step motors uses the stator's bending mode as an operating mode, and its two operating states are determined by the relative position between stator teeth and the standing wave. When stator teeth are between the standing wave peaks (or trough) and the nodal diameter, the motor is in the state of the standing wave driving, and its driving mechanism is the same as the aforementioned standing wave motor. Meanwhile the friction at the interface is active. When stator teeth locate near the wave peak (or trough), it is in the self-correction positioning state.

Self-correction mechanism is shown in Fig. 10.30. Under the action of pre-

pressure F_n, the torsional deformation of the rotor's lobule leads to a circumferential force F_τ, as shown in Fig. 10.30(a), which drives the rotor rotating. When stator teeth are in the rotor slot, the circumferential forces F_τ and F'_τ act at the adjacent two lobules of the rotor, which possess the same magnitude but the opposite directions, and the rotor is no longer rotating to realize the rotor's positioning. The relative sliding during the contact of the stator with the rotor is a necessary condition for the rotor's rotation. As a result, the friction force at the interface is resistance.

Because stator teeth stand in the peak (or trough) is the self-correction state, this type of motors is called as the self-correction peak type step USM. The torque in the self-correction state depends on the torsional angle, which is formed by the torsional deformation of the rotor's lobule turning around the geometric symmetry axis under the action of the stator tooth.

2. Stepping principle

As shown in Fig. 10.29, the step motor with 4 stator teeth, 8 rotor slots and a piezoelectric ring unidirectional polarized with 12 electrodes are designed. In the motor structure, B_{02} operating mode is utilized. To facilitate observation, it is valid to expand the motor and rotor along circumference, as shown in Fig. 10.31.

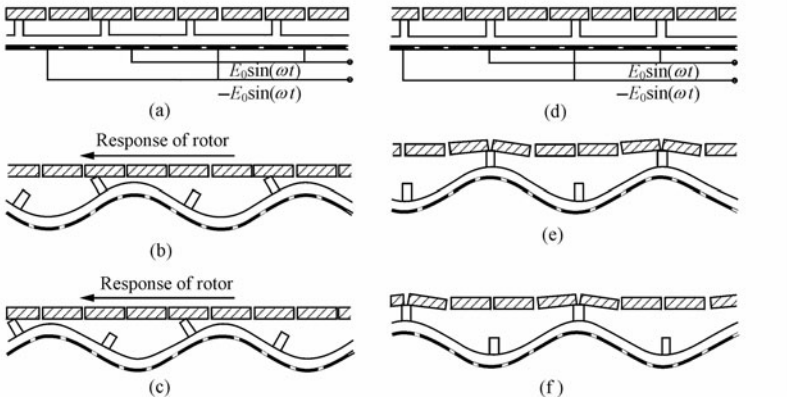

Fig. 10.31 Motion decomposition of self-correction peaks type step USM

The voltage supply is applied to the electrodes in accordance with Fig. 10.31(a). The B_{02} bending standing wave is excited by the piezoelectric ceramic ring. Under the action of stator teeth, the rotor moves along the direction as shown in Fig. 10.31(b) and Fig. 10.31(c). While the rotor slot is in the vicinity of stator teeth, the voltage supply is applied to the electrodes in accordance with Fig. 10.31(d). The B_{02} bending standing wave is excited by the piezoelectric ceramic ring, and at this moment stator teeth are in the place of peaks (or trough). The rotor's lobules are distorted by the effect of stator teeth, which contributes to a circumferential force to make the rotor slot finally to stop just in stator teeth, as shown in Fig. 10.31(e) and 10.31(f). It is the completion of self-correcting posi-

tioning, and the motor's first-step movement has finished at the same time. In this way, alternately changing the electrodes in accordance with Figs. 10.31(a) and (d), the rotor can alternately obtain the both operating states: the standing wave driving and self-correction positioning. Further, the motor step angle is $2\pi/8$.

The step angle of this type of step USMs equals to the angle between the adjacent slots on the rotor, and this is related to the number of rotor's slots. The more the slots are, the smaller the step angle is. The number of stator teeth is related to the use of the operating mode, if we adopt the mode B_{0k}, the number of teeth should be $2k$. Fig. 10.32 shows the self-correction peak type step USM developed by Chunsheng Zhao and Guiqin Wang[4-5]. If using B_{12} vibration mode, the stator is installed with four teeth, and the stator's outer diameter is 40mm, the inner one is 21mm, the height of teeth is 3mm, the stator's thickness is 1.5mm, and its material is 40Cr steel. The rotor is cut into a series of the lobules from the stepping angle, as shown in Fig. 10.32.

As shown in Fig. 10.33, it illustrates the mechanical characteristics of the three kinds of self-correction peak type step USMs (as single-phase driving motors) at the same pre-pressure. Their driving frequency and driving voltage are 32.78kHz and 50V, respectively.

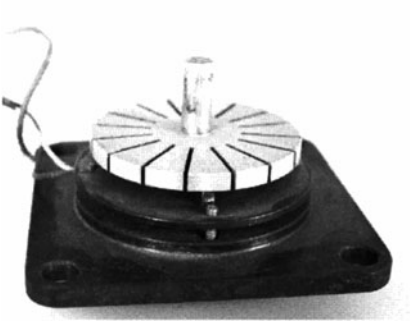

Fig. 10.32 D40 self-correction peak type step ultrasonic motor

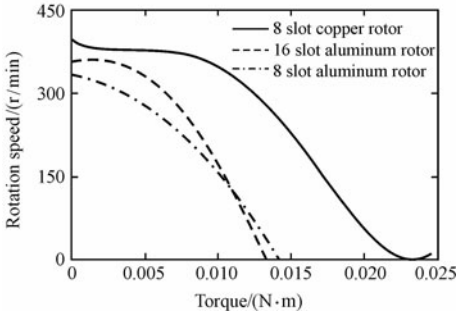

Fig. 10.33 Load characteristic curve

The relevant size parameters are as follows: 8-slot copper rotor's thickness is 1.8mm; 16 slot aluminum rotor's thickness is 3.0mm; a 8-slot aluminum rotor's thickness is 3.0mm. Comparing the characteristic curves, the performance of the USM with a copper rotor is better, mainly because the copper's friction coefficient is larger and machining precision is higher.

3. Features

As the friction at the interface in the two operating states produces the contrary effect, a suitable friction coefficient and a suitable pre-pressure are main factors for operating of the motor, but it is very difficulty to increase a torque in integrated design. In addition, there is another key factor altering the states from the driving state to the positioning state through a switch. Too early switching

will make the rotor to back to original position. On the contrary, switching too late will make the rotor to enter into afterward self-correction region, resulting in multi-step phenomenon.

Corresponding with the self-correction peak step USM, there is another self-correction step USM called the self-correction nodal-line type step USM[36], which also uses the mutual switch of standing wave driving and self-correction positioning to achieve stepping movement. The only difference is that its stator teeth locate at the nodal diameters of operating mode at the self-correction state.

References

[1] C Kusakabe, Y Tomikawa, T Takano, et al. An encoder-less ultrasonic stepping motor using open-loop control system. *Proceedings of 12th Symposium on Ultrasonic Electronics*. Tokyo: Japanese Journal of Applied Physics, 1992, 31(S): 239-241.

[2] T Iijima. Ultrasonic motor using flexual standing wave. *Japanese Journal of Applied Physics*, 1987, 23 (S): 191-193.

[3] O Miyazawa. Drive control unit for an ultrasonic step motor. *US Patent* 5229678, 1993-07-20.

[4] Chunsheng Zhao, Guiqin Wang. Self correction ultrasonic motor using standing wave. *Chinese Invention Patent* 1133265, 2003-12-31.

[5] Guiqin Wang. *Research on Self Correction Ultrasonic Motor Using Standing Wave*. Dissertation for the Degree of Master. Nanjing: Nanjing University of Aeronautics and Astronautics, 1999. (in Chinese)

[6] Chunsheng Zhao, Long Jin. Multiphase stepping ultrasonic motor. *Chinese Invention Patent* 1299180, 2001-06-13. (in Chinese)

[7] Long Jin. *Research on Stepping Ultrasonic Motors*. Post-doctoral Report. Nanjing: Southeast University, 1999. (in Chinese)

[8] V Snitka. Ultrasonic actuators for nanometer positioning. *Ultrasonics*, 2000, 38: 20-25.

[9] Yong Jin, Jifeng Guo, Kehui Ji. Stepping positioning control on ultrasonic motor. *Mechanical and Electrical Engineering*, 2003, 20 (6): 25-29. (in Chinese)

[10] Xiangchen Chu, Zengping Xing, Longtu Li, et al. High resolution miniaturized stepper ultrasonic motor using differential composite motion. *Ultrasonics*, 2004, 41: 737-741.

[11] Jiamei Jin. *Development on Some Novel Ultrasonic Motor*. Dissertation for the Degree of Doctor. Nanjing: Nanjing University of Aeronautics and Astronautics, 2007: 71-77.

[12] Chunsheng Zhao, Jiamei Jin. Frequency stepping ultrasonic motor using standing wave. *Chinese Patent* 1688097, 2005-10-26.

[13] Jiamei Jin, Chunsheng Zhao. Bi-mode alternation stepping ultrasonic motors. *Journal of Nanjing University of Aeronautics and Astronautics*, 2006, 38(5): 600-604. (in Chinese)

[14] Chunsheng Zhao, Jiamei Jin. Linear stepping ultrasonic motor. *Chinese Invention Patent* 1777011, 2006-07-10.

[15] Jiamei Jin, Chunsheng Zhao. A vibrators alternation stepping ultrasonic motor. *Ultrasonics*, 2006, 44(1): 561-564.

[16] Chunsheng Zhao. Ultrasonic motor techniques in the 21st century. *Journal of Vibration, Measurement & Diagnosis*, 2000, 20(1): 7-11. (in Chinese)

[17] Huafeng Li, Chunsheng Zhao. Precise position control of ultrasonic motor using fuzzy control. *IEEE International Ultrasonics, Ferroelectrics, and Frequency Control Joint 50th Anniversary Conference*. Montreal, Canada: IEEE, 2004: 23-27.

[18] Qianwei Chen, Weiqing Huang, Chunsheng Zhao. Measurement of service life of ultrasonic motors. *Journal of Vibration, Measurement & Diagnosis*, 2004, 24(1): 19-22. (in Chinese)

[19] Xiangdong Zhao, Bo Chen, Chunsheng Zhao. Characteristics estimation and optimal design of traveling wave type ultrasonic motor. *Small & Special Electrical Machines*, 2003(5): 13-15, 19. (in Chinese)

[20] Shoushui Wei, Yuling Zhang, Chunsheng Zhao. The application of fuzzy control to USM-actuated position servo system. *Electric Machines and Control*, 2002, 6(3): 218-220. (in Chinese)

[21] Shoushui Wei, Hui Guo, Chunsheng Zhao. A novel method of phase control for ultrasonic motor. *Journal of Southeast University*, 1999, 29(5B): 76-79. (in Chinese)

[22] Jiakui Zu, Chunsheng Zhao. Development of driving and control technique for traveling wave ultrasonic motors. *Small & Special Electrical Machines*, 2004(6): 38-42. (in Chinese)

[23] Zhirong Li, Weiqing Huang, Chunsheng Zhao. Motion analysis and simulation of the stator driving surface of the cylinder sphere ultrasonic motor with multi-degree of freedom. *Mechanical Science and Technology*, 2004, 23(11): 1352-1355. (in Chinese)

[24] Hai Xu, Weiqing Huang, Chunsheng Zhao. One type of linear ultrasonic motor based on the vibration in plane of the plate. *Journal of Vibration Engineering*, 2003, 16(S): 38-40. (in Chinese)

[25] Quanting Liu, Weiqing Huang, Chunsheng Zhao. Linear ultrasonic motor and it's type applications. *Journal of Vibration Engineering*, 2003, 16(S): 25-28.

[26] Weiqing Huang, Guoqing Huang, Chunsheng Zhao. Research on multi-stator linear ultrasonic motor. *Piezoelectrics & Acoustooptics*, 2004, 26(6): 451-453, 459. (in Chinese)

[27] Hai Xu, Chunsheng Zhao. Development and application of linear ultrasonic motors. *China Mechanical Engineering*, 2003, 14(8): 715-717. (in Chinese)

[28] Heling Su, Chunsheng Zhao. Study on the dynamic modeling and simulation of a rotatory type ultrasonic motor with single phase driving circuit using standing wave. *Chinese Journal of Applied Mechanics*, 2003, 20(2): 78-82.

[29] Junbiao Liu, Weiqing Huang, Chunsheng Zhao. A new type linear ultrasonic motor with two degrees of freedom. *Piezoelectrics & Acoustooptics*, 2001, 23(5): 346-358. (in Chinese)

[30] Xiaohong Yuan, Junbiao Liu, Chunsheng Zhao. Study on a new linear ultrasonic motor with standing wave. *Piezoelectrics & Acoustooptics*, 2001, 23(3): 198-201. (in Chinese)

[31] Heming Sun, Shoushui Wei, Chunsheng Zhao. Research on ultrasonic motor using longitudinal and torsional mode. *Journal of Nanjing University of Aeronautics & Astronautics*, 2000, 32(5): 603-607. (in Chinese)

[32] Chunsheng Zhao, Guiqin Wang, Long Jin. A new type of self-correction ultrasonic motor using standing wave. *IEEE Ultrasonic Symposium*, 1999, 2: 671-674.

[33] Chaodong Li, Chunsheng Zhao. A large trust linear ultrasonic motor using longitudinal and flexural modes of rod-shaped transducer. *Proceedings of the* 1998 *IEEE International Ultrasonics Symposium*. Sendai Miyagi, Japan: IEEE, 1998: 691-694.

[34] Chaodong Li, Long Jin, Chunsheng Zhao. The characteristics of hybrid transducer type linear ultrasonic motor with large thrust and large stroke. *Chinese Journal of Acoustics*, 1999, 18(3): 266-271.

[35] Tiemin Zhang, Chunsheng Zhao. Comments on servo control over ultrasonic motors. *Journal of Vibration, Measurement & Diagnosis*, 2001, 21(3): 203-208. (in Chinese)

[36] X Chen, C Kusakabe, Y Tomikawa, et al. Rotor displacement of the ultrasonic motor having an angular displacement self-correction function. *Japanese Journal of Applied Physics*, 1993, 32 (1): 4198-4201.

[37] Chunsheng Zhao. *Ultrasonic Motors Technologies and Applications*. Beijing: Science Press, 2007. (in Chinese)